Epoxy-based composites with size-fractionated waste Areca sheath: an experimental investigation on the macroscopic and vibrational properties

Lijo Varghese, G. C. Mohan Kumar
Department of Mechanical Engineering, National Institute of Technology Karnataka, India
lijovarghese08@gmail.com , http://orcid.org/ 0000-0001-9550-8891
mkumargc@nitk.edu.in, https://orcid.org/0000-0002-7282-7512

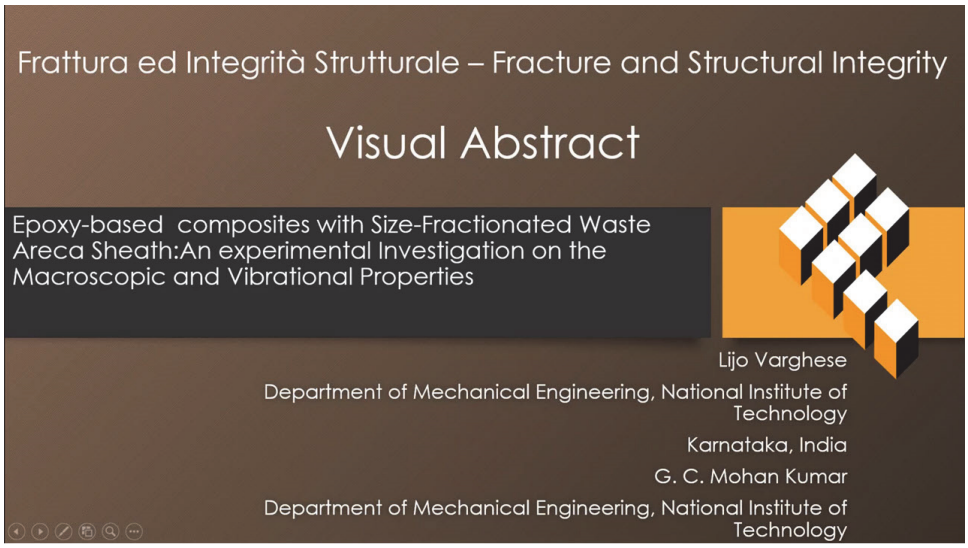

Citation: Varghese, L., Mohan Kumar, G. C., Epoxy-based composites with size-fractionated waste Areca sheath: an experimental investigation on the macroscopic and vibrational properties, Fracture and Structural Integrity, 71 (2025) 49-66.

Received: 17.08.2024
Accepted: 26.09.2024
Published: 08.10.2024
Issue: 01.2025

KEYWORDS. Natural fibres, free Vibration, Natural frequency, Mechanical Properties, Damping factor, Epoxy Composites.

INTRODUCTION

The natural fibre composites present a realistic alternative to synthetic fibre-reinforced composites. Natural fibres offer notable benefits such as higher specific strength, reduced cost, biodegradability, renewability, and superior thermal and acoustic insulation properties [1]. Within a composite material, the reinforcement, often in the form of fibres or particulates, bears the load and inhibits the propagation of cracks within the polymer matrix [2]. Nature, in its abundance, provides the gift of plant fibre, serving as an organic reinforcement in various applications [3]. In recent years, researchers have been proactive in searching for eco-friendly fillers to enhance mechanical properties, leading to the identification of non-wood fibres, commonly referred to as lignocellulosic fibres [4]. Many research revealed that lignocellulosic fibres like jute, kenaf, bamboo, bagasse, hemp, coir, flax, ramie, sisal, et al., have already established their presence in the engineering sector, but they are derived from the plants directly [5, 6]. Hence, recent research has shifted its

focus toward investigating lignocellulosic fibres derived from plant waste [7]. Areca is cultivated extensively in the tropical regions of South Asia for its fruit. In India, Areca thrives in regions such as Kerala, Karnataka, Assam, Tamil Nadu, Maharashtra, West Bengal, and, to a lesser extent, northeastern states [8]. Areca is a perennial and monoecious palm featuring male and female flowers on the same spadix. The cellulose content of areca sheath fibres (66%) suggests that employing them as reinforcement material could yield favorable mechanical properties in composite materials [9]. Therefore, it is suitable reinforcement, which is thrown after its fruit cultivation.

The areca sheath fibre is brittle in nature, and embedding in a polymer matrix in the particulate form helps to improve dimensional stability during the manufacturing process [10]. In particulate form, the reinforcements range from milli- to micro- to nano-sized particles [11]. The strategic addition of varying proportions and sizes of reinforcements actively contributes to improvements in particulate composites' mechanical, thermal, and acoustic properties [12]. Common polymers used with lignocellulosic fibre are polyethylene, polyurethane, epoxy, vinyl ester, etc. Polymer-based composites are gaining attention in many fields, such as construction, automobile, defense, and packaging, due to their tailoring properties[13]. Thermoset polymer, like epoxy, has excellent mechanical properties and is preferred for industrial and household use[14]. The properties of epoxy include low coefficient of friction, rigidity strength, and modulus. Common reinforcements used in epoxy are fly ash, Glass micro balloons, carbon nanotubes, jute fibre, luffa fibre, and wood floor. In one research, Badyankal et al. [15] investigated the effect of fillers like Coconut shell (CS), Saw dust (SD), Kolam (KP), and Fly ash powder in epoxy resin and identified that Coconut shell (CS) fillers exhibit superior mechanical and wear properties compared to other fillers. CS-filled composites show enhanced tensile and flexural strength, improved fiber-matrix bonding, and reduced wear due to higher lignin content. Nowadays, fiber-reinforced and particle-reinforced composites, including micro- and nano-filled epoxy composites, are widely used in research to customize the performance of polymer composites for specific applications [16]. Due to its exceptional properties and widespread use in various areas, it has been selected as the matrix in this work.

The areca fruit husk fibre, when combined with unsaturated polyester resin through hand-laid compression molding, showcased promising results in mechanical tests adhering to ASTM standards. Notably, a composite featuring a 40% weight ratio of areca husk fibre exhibited superior specific tensile strength compared to an unsaturated glass fibre polyester composite [17]. Another investigation on areca nut husk fiber shows that when it is mixed with mortar at 0.5%, it enhances the mechanical properties and effectively mitigates shrinkage. However, higher areca nut husk fiber content increases porosity, though the overall strength remains above the control mix [18]. Another research into particulate composites, incorporating sunflower husk, hazelnut shell, and walnut shell in epoxy at different weight percentages, unveiled those reinforcements with lower aspect ratios displayed superior hardness and stiffness, owing to the lesser introduction of voids into the composites compared to higher aspect ratio reinforcements [19]. Investigations on epoxy composites reinforced with moringa oleifera fruit pods highlighted the advantages of employing pulverized particulate moringa oleifera over calcined counterparts, particularly in achieving superior fibre and resin bonding [20]. Similar research on bamboo-epoxy composites incorporating clamshell as a filler material revealed that adding clamshell reduces the void percentage while increasing the composite's density and hardness [21]. Investigation done on epoxy resin composites reinforced with wood apple shell particles has demonstrated significant enhancements in their mechanical and tribological properties, including tensile strength, flexural strength, and erosive wear resistance. Dynamic Mechanical Analysis reveals that increasing the weight percentage of wood apple shell particles improves viscoelastic stiffness [22]. Research on polypropylene composites incorporating Ponderosa pine wood flour revealed that increasing the aspect ratio of wood flour led to enhanced tensile and flexural strength and modulus, while an increase in particle size correlated with increased notched specimen impact energy but decreased unnotched specimen impact energy [23]. Another research study of short, randomly oriented sisal and banana fibres in polyester composites reveals that the free vibration characteristics of composites are notably affected by fibre weight percentage and fibre length [24]. Researchers explored the free vibration and damping characteristics of hybrid composites made from short-fibre chopped strand mats, clay, and vinyl ester. They found that the dispersion of nano clay significantly improves the internal damping properties of these composites [25]. Another study found that adding wire mesh and BaSO4 to aloe vera, flax, and hemp epoxy composites increased tensile and flexural strength, hardness, and natural frequency. The composite with both wire mesh and BaSO4 showed the best performance [26]. The literature on natural fibre composites is exciting; however, it appears that studies are missing on the use of waste areca sheaths to prepare composites, and limited research is available on the vibrational analysis of areca sheath composites for construction, automobile panel materials.

This study explores the potential of areca sheath micro-sized particulates in composite materials, addressing a key research gap. Three different micro-sized particulates of areca sheath—coarse, fine, and very fine(AS-C,F, VF)—were systematically prepared from the sheath for this purpose. Subsequently, AS-C, AS-F, and AS-VF-reinforced epoxy composites were fabricated using varying weight fractions (ranging from 5% to 20%) of these particulates. The study investigates the influence

of these particulates as reinforcement agents, with a comprehensive evaluation of their mechanical properties, including tensile, flexural, impact, hardness, and vibrational tests. The objective is to develop a composite material with enhanced properties suitable for diverse applications, particularly in infrastructure and automobile panel materials. The originality of this research lies in the novel use of areca sheath particulates in varying sizes and their systematic impact analysis, which has not been extensively explored in previous studies.

MATERIALS & METHOD

Materials

Areca sheaths were sourced from a local farm in Mangalore, India. The resin employed in this study consisted of Epoxy (L-12) and hardener (K-6) supplied by Atul Ltd., Gujarat, India, as shown in Fig .1. L-12 epoxy resin offers an affordable option with excellent resistance to environmental degradation, enhanced performance, and durability against thermal and water degradation. It's particularly well-suited for constructing building panels, especially for facades. The chemical composition of this resin is known as Diglycidyl ether of bisphenol-A [27], which is synthesized through the reaction between epichlorohydrin and bisphenol-A. Its structure is based on the condensation reaction of bisphenol-A and epichlorohydrin, resulting in a linear polymer chain with epoxy groups at each end. The hardener K-6 is a light-yellow aliphatic polyamine with a chemical name triethylene tetra amine designed for curing epoxy resin at room temperature. K-6 hardener is a useful and reliable curing agent that balances mechanical strength, thermal stability, and chemical resistance when used with compatible epoxy resins. It is widely used in engineering applications, including composite manufacturing and adhesives.

Figure 1: (a) Areca sheath(b) L-12 Epoxy and K-6 Hardener.

Methods: Fibre Extraction

The collected areca sheath from farmland has been washed and soaked in water for a few days; as a result, the fibre extraction becomes easy. The fibres were removed using a metal brush and chopped into 10 to 50-mm lengths. It was then sun-dried and later in an incubator at 70°C for 24 hours to remove all moisture. The density of the areca sheath particulate was determined in accordance with ASTM standard D792. The different lengths of areca sheath fibres have been taken for density measurement. The collected areca sheath fibres were cleaned with fresh water to eliminate dirt. Subsequently, these cleaned areca sheath fibres were stored and dried in an incubator at 40°C. Then, a mechanical pulverizer was employed to prepare particulates, followed by filtration using sieves with different mesh sizes (30, 50, 115, and 200) to obtain particulates of varied sizes. These sieves were arranged in a specific order: 30 mesh (600 μm) on top, followed by 50 mesh (300 μm), 115 mesh (150 μm), 200 mesh (75 μm), and base at the bottom. The coarse particles were collected in a 50 mesh sieve, while the fine particulates were collected in a 115 mesh sieve, and the very fine particulates were collected in a 200 mesh sieve; the remaining particulates passed through the sieve and collected in the base. The sizes of the particulates were categorized based on the mesh size of the sieves. The particulates collected in a 50 mesh sieve were classified as AS-C (300-600 μm), those in the 115 mesh sieve were labeled as AS-F (150-300μm), and the ones in the 200 mesh sieve were considered AS-VF(75-150 μm), as illustrated in Fig.2.

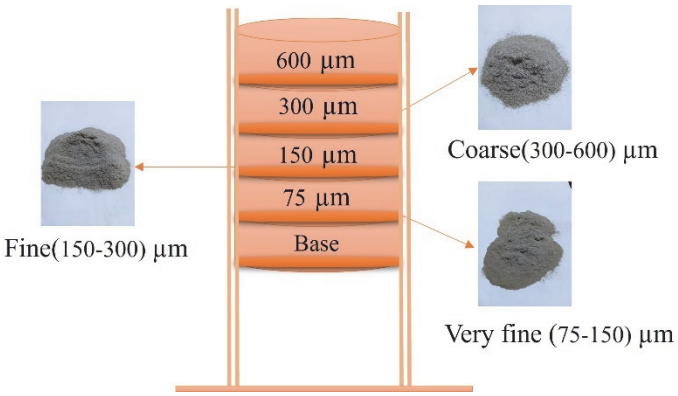

Figure 2: Sieve setup for different areca sheath particulates.

Methods: Particle size analysis and morphology classification

A Leica optical microscope measured the geometric shape and aspect ratio of AS-C, AS-F, and AS-VF particulates obtained from a mechanical pulverizer. This process involves sequentially placing individual particulates onto a microscope stage, ensuring that the stage is cleared before each placement. Next,the light was turned on, and imaging began with the lower lens(4), with magnification progressively increasing to (500) using the higher lens. After image capture with a Leica optical microscope, aspect ratio measurements were conducted using ImageJ software. About 50 particulates in AS-C, AS-F, and AS-VF particulates have been measured for maximum and minimum dimensions.

Methods: Composites preparation

Areca sheath particulates were ground into coarse, fine, and very fine sizes. To make the composite, the particulates were mixed with epoxy resin, and a hardener was added. First, a measured amount of epoxy and particulates was mixed in a beaker using a mechanical stirrer at 710 rpm for 50 minutes. After that, the hardener was added, and the mixture was stirred for another 8 minutes at 510 rpm. The mixture was then poured into silicone rubber molds to create a test specimen according to ASTM standards. The specimens were cured for 24 hours to harden. Once cured, they were carefully removed from the molds. Each specimen was labeled as Ep/AS-C/5 (Ep/AS stands for Epoxy/Areca Sheath, C stands for coarse, and 5 indicates the weight fraction of areca sheath). A specimen without any reinforcement particulates was also made. The details of all 12 specimens with different particulates are shown in Tab. 1.

	Weight fraction % of Areca Sheath particulates with Epoxy			
	5	10	15	20
Coarse	Ep/AS-C/5	Ep/AS-C/10	Ep/AS-C/15	Ep/AS-C/20
Fine	Ep/AS-F/5	Ep/AS-F/10	Ep/AS-F/15	Ep/AS-F/20
Very fine	Ep/AS-VF/5	Ep/AS-VF/10	Ep/AS-VF/15	Ep/AS-VF/20

Table 1: List of Specimen with different proportions

Physical Properties of Composites

The density of the composites was determined according to ASTM standard D792, using Archimedes' principle to measure the mass and weight of the specimens. Square specimens of 20 × 20 mm were prepared for density measurement, with distilled water as the immersion fluid at room temperature. The mass of each specimen was first measured using a digital balance with milligram precision. The specimen was then immersed in water, and its mass was measured again. The density of the composite specimen was calculated using the formula:

$$Density = \frac{\text{mass of the specimen in air}}{\text{mass of the specimen in air} - \text{mass of the specimen in water}} \quad (1)$$

Tensile investigation of composites

For the tensile test, composite specimens were prepared following the ASTM D3039 standards. The tests were conducted using the universal testing machine (UTM), ZWICK//ROELL Z020, equipped with a 10 kN load cell, as depicted in Fig. 3(a). The specimens were checked for cross-sectional area, and each prepared sample was placed individually in the

machine's jaws. The test was carried out at a 2 mm/min crosshead speed. The specimens were pulled until they broke, and the breaking point was identified. Final length, width, and thickness are measured from the vernier caliper. Multiple samples were prepared, and three specimens were tested for each set. The lateral strain was then calculated based on the final width of the specimen. Finally, the Poisson's ratio was calculated for each specimen. These specimens' average values were presented to ensure reliable and representative data.

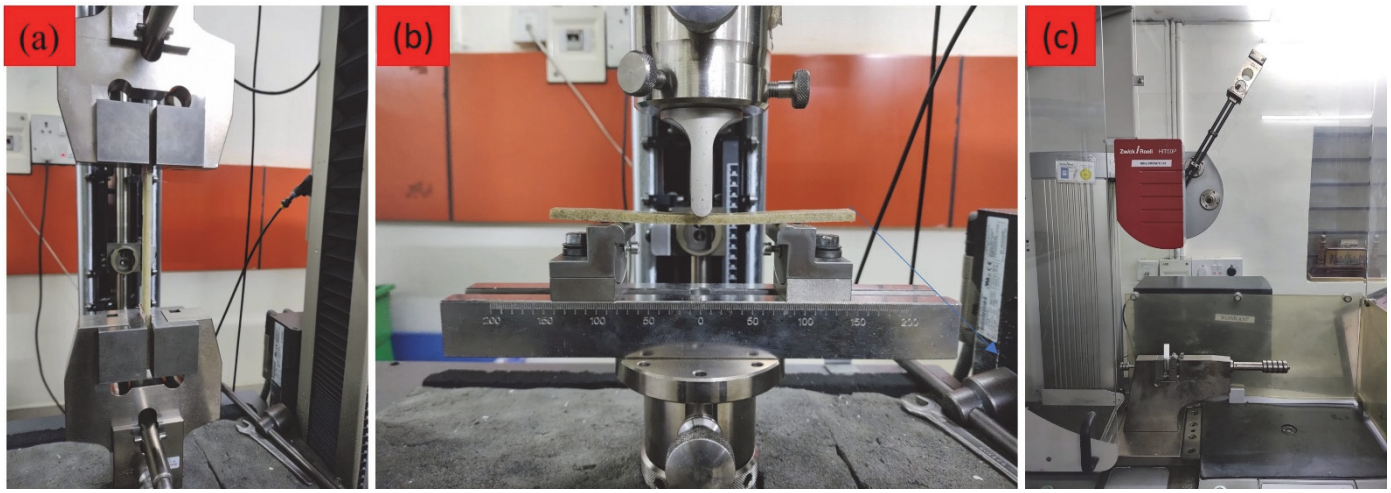

Figure 3: Experimental setup for (a) Tensile test, (b) Flexural test and (c) Impact test.

Flexural investigation of composites

The three-point bending test method was employed to determine the flexural strength and modulus of the developed composites. Following the ASTM-790 standard, the flexural test was conducted using a universal testing machine (UTM), ZWICK//ROELL Z020, equipped with a 10 kN load cell and the specimen, with beam-like dimensions of 150 x 12.7 x 3 mm, as depicted in Fig. 3(b), was subjected to a load applied vertically at the center of the specimen until the specimen was broken. An extreme position was utilized as a sample support member during testing.

Impact test of composites

The Izod impact test was conducted to evaluate the impact resistance of the composites as per ASTM D4812-99 standards. In this test, an unnotched specimen, as per specifications, was securely fixed in the jaws, and a pendulum struck the specimen, measuring the energy absorbed by the specimen during fracture. The test apparatus used for this purpose was the ZWICK/ROELL Z020 HIT50P and specimens as illustrated in Fig. 3(c).

Hardness Investigation of Composites

The Shore-D hardness test method specified in ASTM D-2240 was employed to measure the hardness of the composites. A durometer indenter was attached to a spring and indented at three different places on the composites. The average value of these measurements was taken for the analysis of composites. The Shore-D hardness test method is particularly suitable for polymer composites, as the indentation depth is directly proportional to the hardness measurement, allowing for easy and accurate measurement.

Free Vibration test of composites

Experimental modal analysis is utilized to extract fundamental parameters such as natural frequency and modal damping relating to the dynamic behavior of structures. Experimental modal analysis is conducted using an impulse hammer test. The schematic diagram in Fig.4 illustrates the setup for the free vibration test. The study analyzes the natural frequency and modal damping factors associated with the various particulate composite materials, including size factors and different weight fractions. The impact of the size factor of areca sheath particulate on composites and the influence of weight fraction composites are examined. These analyses are performed on beam-like composite specimens under clamped-free boundary conditions configurations. To determine the natural frequency of a particulate composite specimen measuring 210 × 12.5 × 4 mm, fixed on a rigid support, a single-axis accelerometer (Kistler 8730A500) is fixed with the specimen using wax. The impact or displacement signal is then captured by the accelerometer and transmitted to the 4-channel data acquisition system. The time domain signal is transformed into a frequency response signal using the Fast Fourier Transform (FFT) algorithm.

Within the LabView software, the frequency response values are directly measured for various particulate composite specimens, and the damping factor value is evaluated by the half-power bandwidth method.

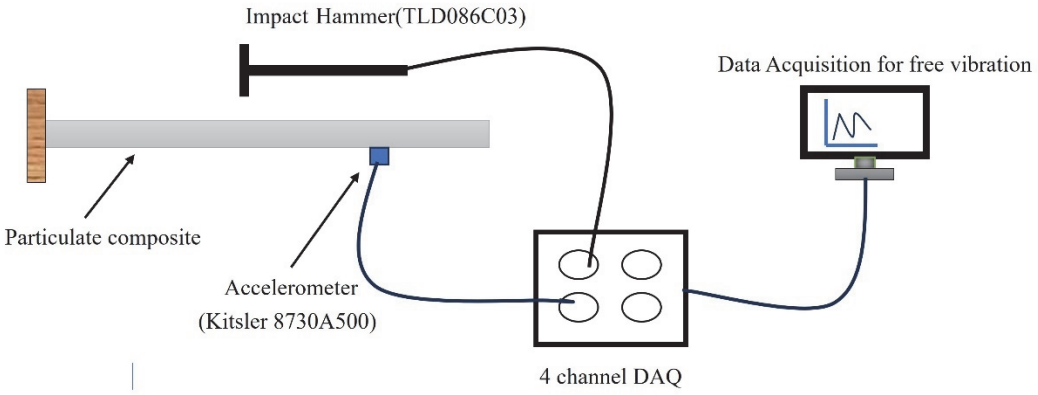

Figure 4: Schematic representation of free vibrational experimental setup

Fractographic investigation of composites

In this analysis, the surface of the fracture in the tensile failure of different specimens was investigated to assess the composites' behavior directly. Studying fractography provides in-depth knowledge of the fracture mechanism, enabling a better understanding of the material's behavior under specific conditions. SEM (Scanning Electron Microscope) images were captured using the ZESIS, EVO MA18, Germany instrument at 10 kV. Since the samples were nonconductive, a gold film was coated using a sputtering machine to make them conductive. After gold coating, the samples were placed in the SEM machine in a pressurized nitrogen environment for scanning.

RESULTS AND DISCUSSION

Fibre density

The average result obtained from five samples of different lengths indicates that the areca fibre densities are approximately 0.91 g/cm³. Subramanyam et al. [28] measured the density of areca fibre as 0.90 g/cm³, whereas Nayak et al. [29]. reported a density of areca sheath fibre as 1.040 g/cm³. This difference may be attributed to fibre voids, growth location, maturity, and porosity.

Particle size analysis and morphology classification

Particle size distribution from the sieve shaker conveys the percentage of particulates retained on different-sized sieves, as illustrated in Fig.5. A maximum weight % distribution was attained in the range of AS-C particulates. The optical images present three distinct pulverized particulate sizes, as shown in Fig.6.

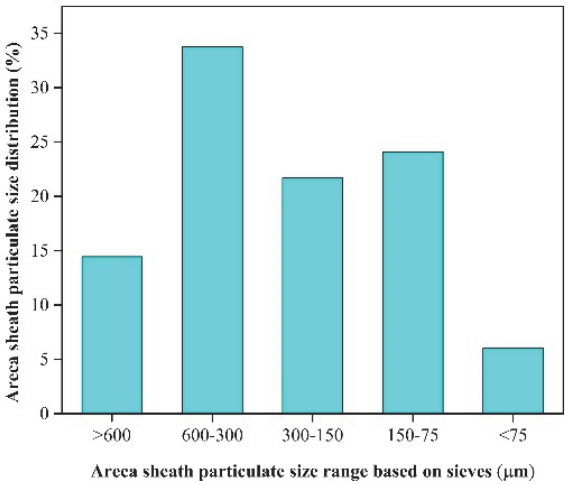

Figure 5: Particle size distribution based on the mass retained in the sieves

These images highlight the geometric shape of the particulates. As the particulate size decreases due to the pulverization process, the morphology undergoes a transformation from evan flat fibres to irregular flat surfaces. The shape of AS-C, AS-F, and AS-VF resembles the structure of chopped fibres. Based on the ASTM standard F 1877-05, they come under sharps and shards of rectangular fibres. The aspect ratio of the AS-C and AS-F particulate sizes surpass that of the AS-VF particulate sizes. Its difference is very small, as shown in Fig.6. The aspect ratio of the particles is the ratio of the longest dimension to the shortest dimension of the particles. These particulate aspect ratios were measured using ImageJ software. The aspect ratio maximum range for the AS-C comes at 3-4; for the AS-F, its maximum range is 2-3; and for the AS-VF, it spans from 1-2.

Figure 6: Optical images of areca sheath particulates.

A natural fibre's performance in composite material depends mainly on its aspect ratio, fibre-matrix interaction, fibre surface area, chemical composition, growing condition, and how that fibre or fibre/matrix performs under a given set of environmental conditions. The aspect ratio of natural fibre should be optimum, and then the stress transfer should be maximum in the particulate composite. If the aspect ratio value is less than its optimum or greater, the stress value decreases and is added without any advantages in composites.

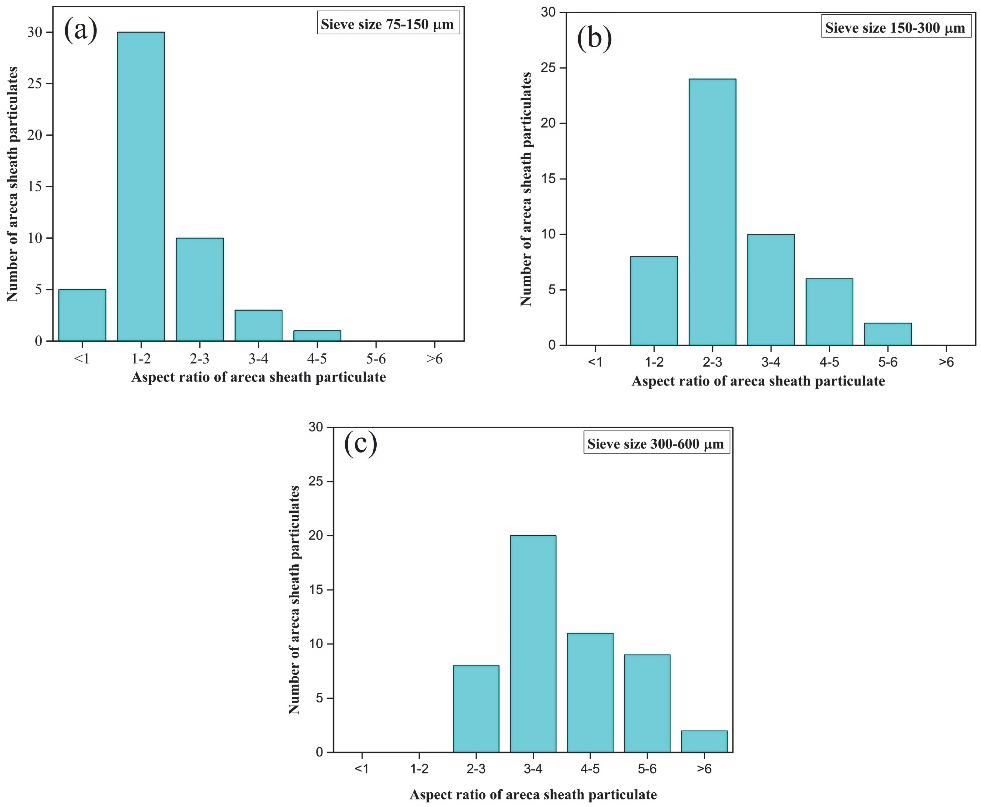

Figure 7: Aspect ratio of areca sheath particulate of (a) Very fine (b) Fine (c) Coarse

Density of particulate composites

The density of particulate composites was measured and represented in Fig.8. However, it is noteworthy that the rate of density reduction is more pronounced in the very fine particulate areca sheath composites(Ep/AS-VF), potentially indicating a higher presence of voids in these composites because as the surface area of particulate increased, the resin could not cover its surface completely. This might show that the density of Ep/AS-VF is low compared to fine particulate areca sheath composites (Ep/AS-F) and coarse particulate areca sheath composites (Ep/AS-C) at high-weight fractions. For the Ep/AS-VF, the density started at 1.156 gm/cm3 at 5% weight fraction and gradually decreased to 1.0688 gm/cm3 as the weight fraction increased to 20%. The density of Ep/AS-VF/20, Ep/AS-F/20, and Ep/AS-C/20 were 1.0688, 1.091, and 1.105 gm/cm3. This is because as areca sheath particulate size decreased, smaller particulates agglomerated and became bigger. Reinforcement of agglomerated particulates has the ability to create void and discontinuous phases within the epoxy resin.

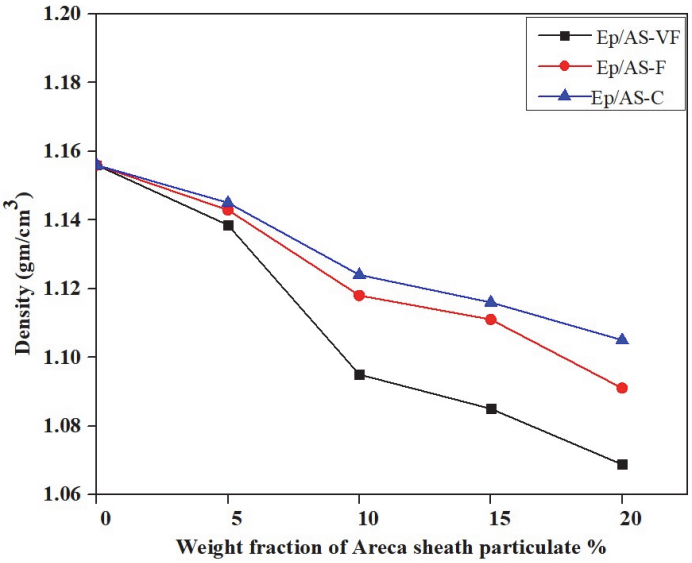

Figure 8: Influencing of Weight fraction on the density of composites.

Tensile test of particulate composites

This study utilized three different particulate sizes—AS-C,AS-F and AS-VF—to prepare composites with a 5% to 20% weight fraction of areca sheath particulates. Stress-strain graphs for different particulate composites are presented in Fig.9. The graphs reveal that the composites failed under tensile loading through brittle fracture. The Ep/AS-VF failed earlier than the Ep/AS-F and Ep/AS-C. These tensile failures depend on many factors, such as particle size or aspect ratio, concentration, adhesion at the particle-matrix interface, and the composite's microstructure[30]. AS-C size has a higher aspect ratio than AS-F and AS-VF sizes, which contributes to better load-transferring capacity in Ep/AS-C.

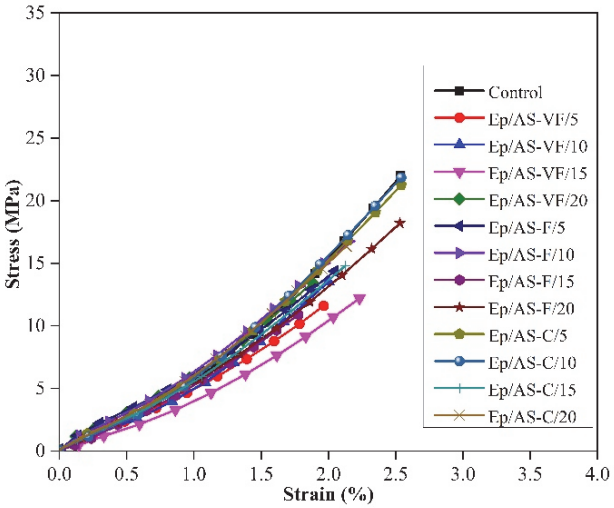

Figure 9: Stress-strain curve of particulate composites.

However, the tensile strength values were lower than the control in Ep/AS-F and Ep/AS-VF. This discrepancy is attributed to insufficient stress transfer from resin to reinforcement. In contrast, the tensile strength of the Ep/AS-C/10 specimen was 9 % higher than the control, showcasing that natural fibre with good aspect ratio particulates used as filler in epoxy resin increases tensile strength at 10% weight fraction . Stark et al[23]. reported that wood flour with the highest aspect ratio in polypropylene resin resulted in the highest tensile strength and modulus. The strain decreases as the weight fraction of the areca sheath particulate increases in Ep/AS-F and Ep/AS-VF compared to the control specimen. This is because of the increase in AS-F and AS-VF in epoxy resin, resulting in the brittleness of particulate composites, further decreasing the lateral strain.

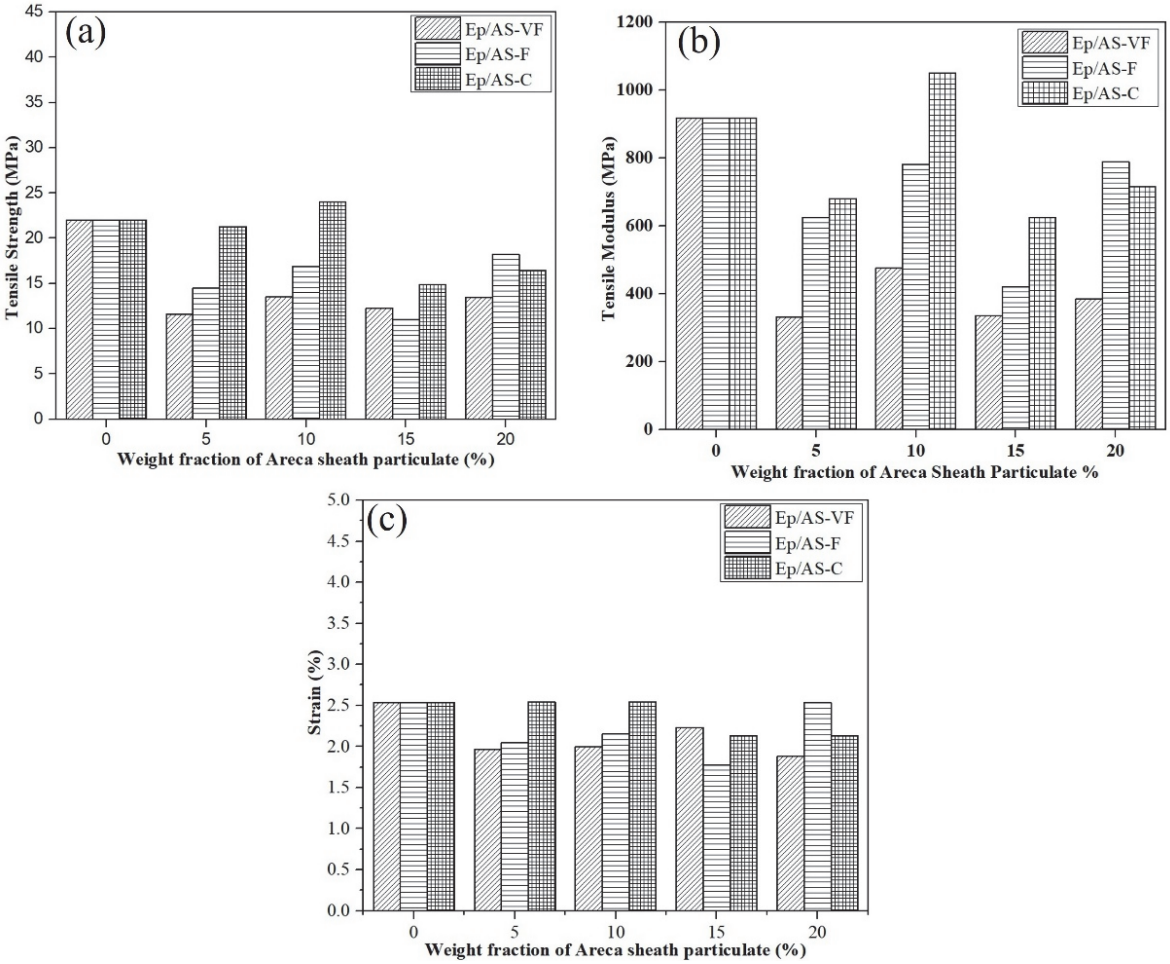

Figure 10: Tensile Strength ,Tensile modulus and Strain in Ep/AS composites

However, the tensile modulus values were higher for Ep/AS-C/5 specimen to Ep/AS-C/10 specimen particulate composite than for the Ep/AS-C/15 specimen(shown in Fig.10). In particular, Ep/AS-C/10 specimen exhibited a 14.37 % higher tensile modulus than the control, measuring 1050MPa compared to 918 MPa in the control. This is because the Ep/AS-C/10 specimen has the most effective load transfer between AS-C and epoxy resin. The highest aspect ratio rendered by AS-C might be the reason for the effective load transfer between them. The SEM images of the tensile tested Ep/AS-C/10 specimen are shown in Fig. 15(b), which show better bonding between resin and AS-C. The Ep/AS-C/5 specimen had a tensile modulus value of 680 MPa, which was 25.9 % lower than the control. However, the tensile modulus values the Ep/AS-VF series, the Ep/AS-VF/5 specimen exhibits a tensile modulus of 332 MPa.This suggests that adding AS-VF decreases the stiffness of the composite. However, the Ep/AS-VF/10 specimen shows a slightly higher tensile modulus of 475 MPa, which is still a lower over control. In contrast, the Ep/AS-VF/15 sample has a tensile modulus of 335 MPa, representing a decrease in tensile modulus again compared to the control. In the Ep/AS-F series, the same trend is followed as Ep/AS-F because the low aspect ratio rendered by AS-F might be the reason for this low load transfer between them. Furthermore, the tensile modulus of Ep/AS-C/10 specimen exceeded the values of Ep/AS-F/10 and Ep/AS-VF/10 specimens. This reduction might be due to the specimen's brittleness, which reduces the load-bearing capacity and ductility.

Flexural test of particulate composites

The influence of the areca sheath particulate on composites' flexural strength and flexural modulus follows a similar trend to the tensile properties, as shown in Fig.11. The Control, Ep/AS-F/5, Ep/AS-F/20, and Ep/AS-C/5 composites specimen flexural strength values as 31.4,37.99,32.451 and 32.82 MPa while flexural modulus values as 2642.65, 2928.29, 2672.36, and 3043.29 MPa, respectively. The maximum flexural strength obtained at the Ep/AS-F/5 specimen and modulus obtained at Ep/AS-C/5 specimen is 20.76% and 15.16% higher when compared to the control specimen. The AS-C, and AS-F has a high aspect ratio compared to the AS-VF sizes, which might bind with the resin together and transfer stress from resin to particulate effectively, resulting in improved flexural properties at 5 and 10 % weight fraction. In each series, the flexural properties tend to decrease after a 10% weight fraction of resin and reinforcement. This might be due to bonding decreases after this threshold, which impacts the overall flexural performance of the particulate composite. Migneault et al[31].reported that the higher the aspect ratio of fibre in resin, the better the stress transfer from resin to fibre compared to the lowest aspect ratio of fibre in resin. However, if the weight fraction is increased beyond 10 %, its strength and modulus decrease because wettability is decreased, and a discontinuous phase is created, which weakens the composites. For Ep/AS-VF series Ep/AS-VF/5 and Ep/AS-VF/10 specimen flexural strength and flexural modulus were 29.28,29.72 MPa, and 2606.53,2426.20 MPa, which is the maximum in its Ep/AS-VF series but lower than control, this shows that lower aspect ratio can't transfer load from resin to reinforcement effectively.

Similarly, Ep/AS-F/5 and Ep/AS-C/5 have shown the highest value of flexural strength and flexural modulus. Natural fibre particulate composite's flexural strength and modulus depend on various factors, including the aspect ratio of fibre particulates, fibre weight percent, fibre weight fraction, surface area of fibre, fibre cellulose content, and the bonding between the filler and resin[32]. Furthermore, the inclusion of areca sheath particulate in epoxy resin shows better results in 5 % weight fraction at each category of particulate.

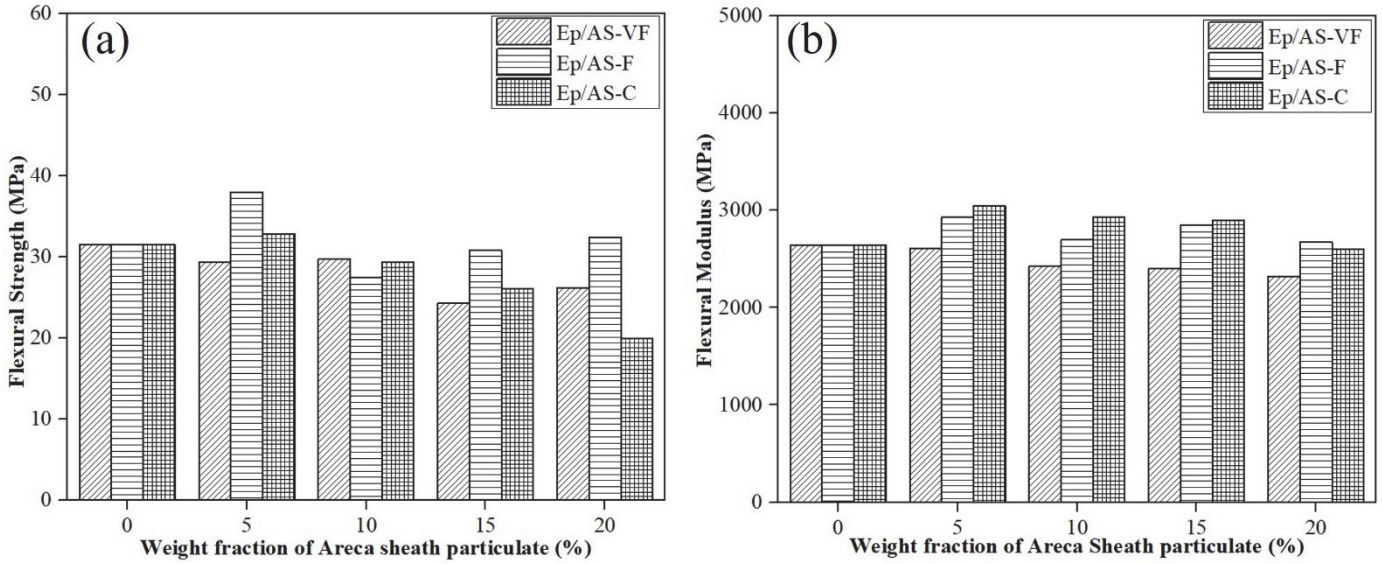

Figure 11: Flexural Strength and modulus in Ep/AS composites

Impact test of particulate composites

The energy that caused the dynamic failure of composites was measured using Izod impact tests. The crack propagation and initiation energy were evaluated using a notched and unnotched Izod specimen. Crack initiation happened at the composites due to the stress concentration of particulates of different weight fractions. The impact energy results of the unnotched specimen are shown in Fig.12(a), the impact strength properties of various particulate composites were compared against control, which has an impact energy of 23.44 J/m. In the Ep/AS-VF series, the Ep/AS-VF/5 specimen showed a noticeable improvement with an impact energy of 29.5 J/m, approximately a 25.89% increase over control. However, the Ep/AS-VF/10 specimen increased to 34.54 J/m, indicating an impact energy enhancement of 47.38 %. The Ep/AS-VF/15 specimen exhibited a moderate improvement, with an impact energy of 24.92 J/m, representing a 6.31% increase over the control. This trend reversed with the Ep/AS-VF/20 specimen, significantly decreasing to 19.89 J/m.In the Ep/AS-F series, the Ep/AS-F/5 specimen had an impact energy of 25.6 J/m, which is a 9.22% increase from the control, suggesting that 5% particulate content might strengthen the composite. The Ep/AS-F/10 specimen similarly demonstrated a significant

improvement, reaching 34.78 J/m, 48.38% higher than the control. Conversely, the Ep/AS-F/15 and Ep/AS-F/20 specimens had an impact energy of 20.65 J/m and 19.92, an 11.90% and 15.01 %decrease from control. The Ep/AS-C series exhibited the most substantial enhancements. The Ep/AS-C/5 and Ep/AS-C/10 specimens, with an impact energy of 44 and 54.7 J/m, represent an 87.75% and 133.24% increase from control. However, the Ep/AS-C/15 specimen significantly increased to 39.29 J/m, a 67.63% improvement. The Ep/AS-C/20 specimen, with an impact energy of 20.77 J/m, showed a minor decrease of 11.39%. Stark et al[23]. conducted a study on wood-flour-filled polypropylene composites; the results reported that unnotched impact energy appeared to increase with the sizes of wood flour in polypropylene. For a high aspect ratio at lower particulate contents (e.g., 5-10%), the bonding between the epoxy resin and the particulates can be strong, resulting in improved impact energy due to effective stress transfer from the matrix to the particulates. This is evident in the initial improvement in the Ep/AS-F/5 to Ep/AS-F/10 and Ep/AS-C/5 to Ep/AS-C/10 specimen. At the same time, for low aspect ratio, the trend is similar,for instance, the Ep/AS-VF series shows significant improvements at low particulate weight fraction (5-10%), indicating that the particulates used in this series are particularly effective at reinforcing the epoxy resin without causing detrimental effects like agglomeration or poor bonding.

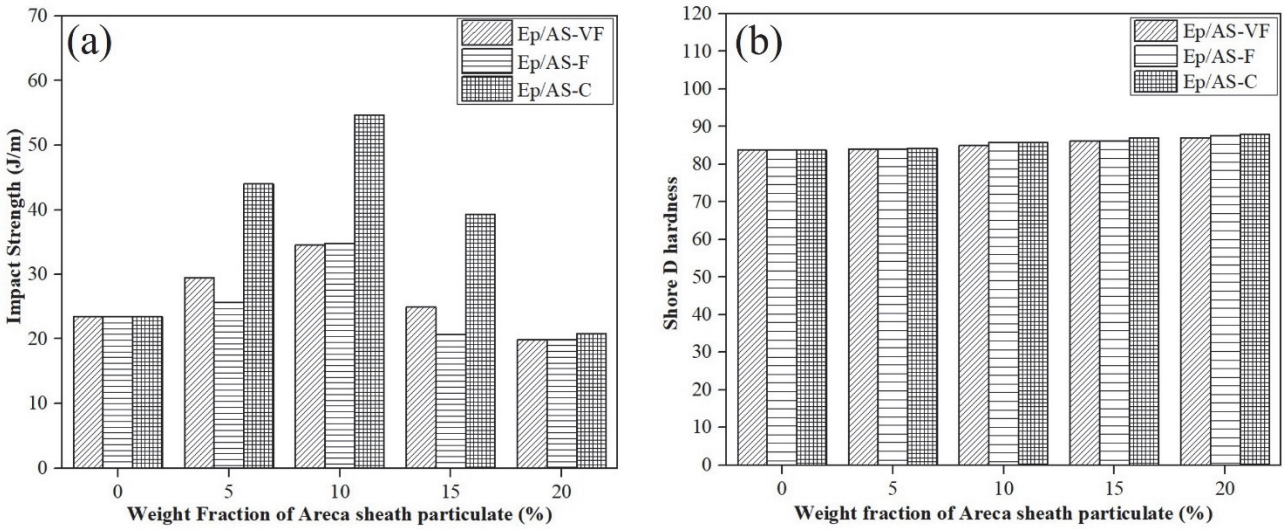

Figure 12: Impact Energy and Hardness in Ep/AS composites.

Hardness test of particulate composites

The influence of the areca sheath particulate size on the hardness of the areca sheath particulate composite is shown in Fig.12(b). As the percentage of areca sheath particulate in epoxy increases, the hardness exhibits an ascending trend as the weight fraction of areca sheath particulate increases. The hardness of Ep/AS-C/5, Ep/AS-C/10, Ep/AS-C/15, and Ep/AS-C/20 composites specimen calculated from shore D methods was 84.2, 85.8, 87, and 88, respectively in the control specimen, its value is 83.8. The maximum value is obtained in Ep/AS-C/20 . The increase in shore D hardness is because as the weight fraction of areca sheath particulate increases in epoxy resin, the penetration depth of the indenter decreases in the specimen. Compared to Ep/AS-C/20, the hardness of Ep/AS-VF/20 and AS-F/20 specimen values is 87 and 87.6 decreased, but no statistical difference was observed.

Natural frequency of particulate composites

The setup of the impact hammer test and typical time and frequency response for a control specimen, as shown in Fig.13(a) & (b), reveals clear peaks in the frequency response curve that indicate the natural frequencies of the control specimen. The natural frequency of various particulate composites was compared to control, which has a natural frequency of 22 Hz. This baseline allows us to evaluate the effects of adding different types and amounts of particulates on the vibrational behavior of the composites.Fig.14(b) illustrates the influence of aspect ratio and weight fraction on particulate composites' fundamental natural frequency under clamped-free boundary conditions. The results indicate that the aspect ratio of the areca sheath particulates significantly influences the particulate composites natural frequency. Specifically, the Ep/AS-C category exhibits a higher natural frequency than other particulate composites, likely because its aspect ratio is higher than other AS-F and AS-VF. At the same time, 10 % weight fractions particulate composites in each category show better natural frequency than lower weight fraction particulate composites such as Ep/AS-VF/20 show 8.33 % higher than Ep/AS-VF/5 similarly, Ep/AS-F/20 shows 8.69 % higher than Ep/AS-F/5. At the same time Ep/AS-C series showing opposite trends

Ep/AS-C/5 shows 8 % higher than Ep/AS-C/20. Ep/AS-C/10 and Ep/AS-F/10 have natural frequencies of 30, and 28 Hz, which is 36.36,27.27 % higher than the control specimen, which is 22 Hz. Similarly, Ep/AS-VF/10 has a 28 Hz natural frequency, which is again 27.27% higher than the control specimen; this should be due to the optimum bonding in the Ep/AS-VF series.

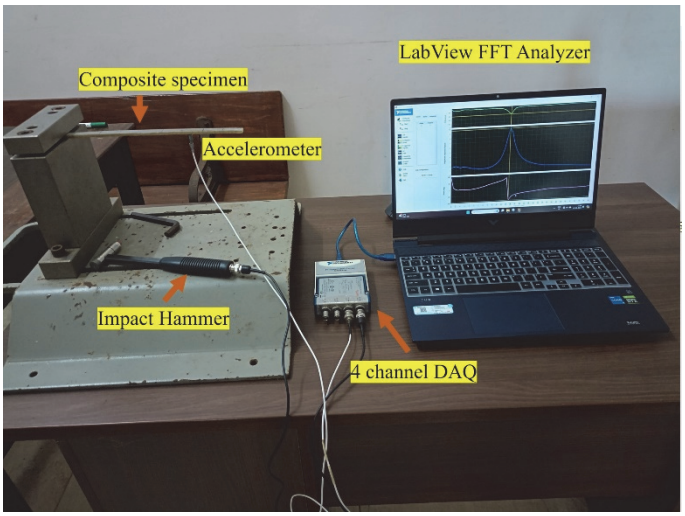

(a)

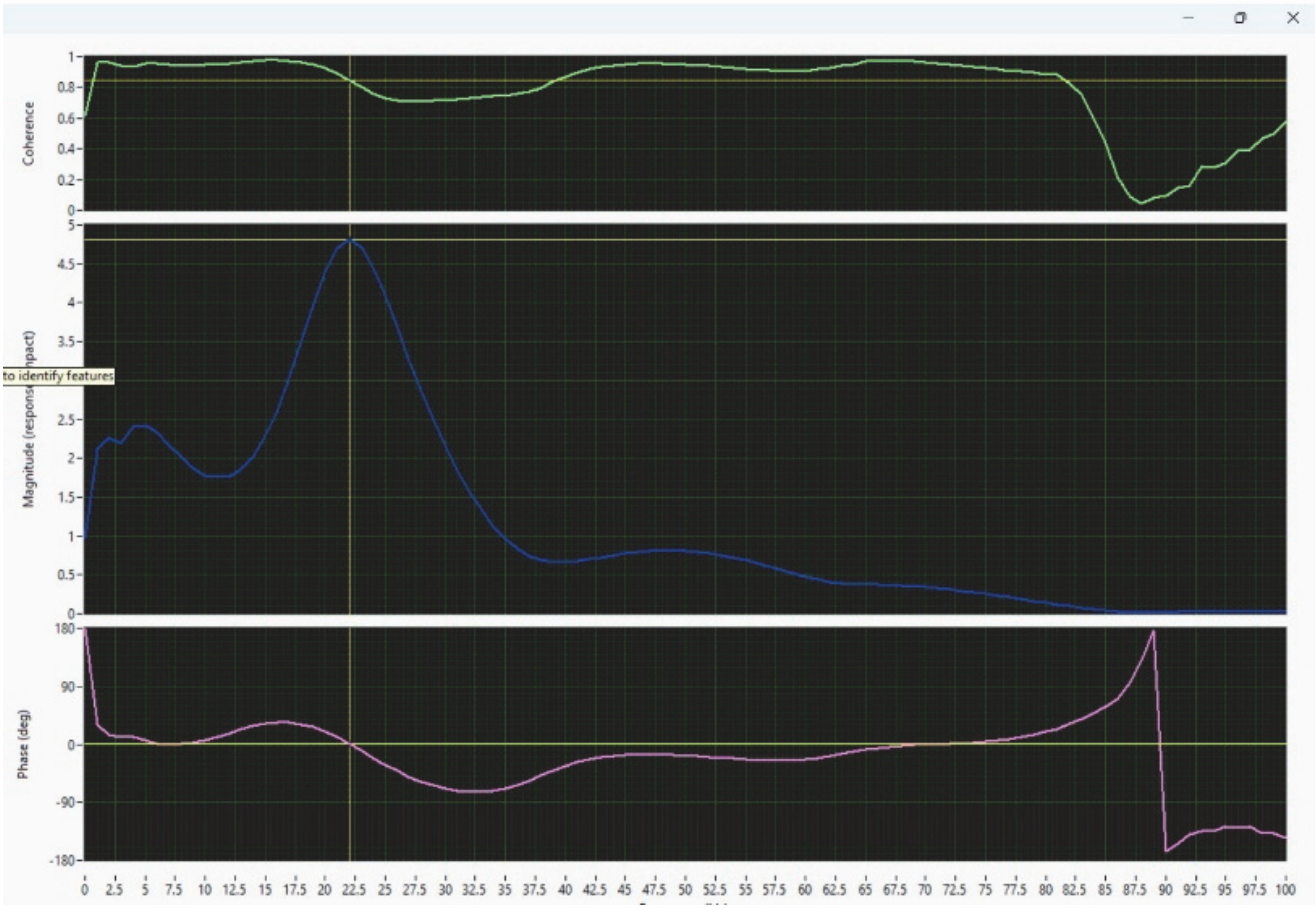

(b)

Figure 13: (a) Experimental setup (b) control specimen time-frequency of composites.

Damping factor of particulate composites

The graph in Fig. 14 (a) is used to find damping factor values using the half-power bandwidth method. This figure shows how to find the half-power points by seeing where the line crosses the Frequency Response Function (FRF) curve. A is the

highest point on the curve. The difference in frequency ($\omega_1 - \omega_2$) values where the curve is cut by a horizontal line drawn at A/$\sqrt{2}$ below the peak. These half-power points help calculate the damping factor. The damping factor for various particulate composites is shown in Fig.14(c). The control, Ep/AS-VF/5, Ep/AS-F/5, and Ep/AS-C/5 show damping factor value has 0.1956, 0.10416,0.1086 and 0.11.The damping factor at lower weight fraction shows a lowest value because the greater weight of resin present in the lower weight fraction of areca sheath particulates composite, which dissipates less energy. For the same weight fraction content(15%) in each category, particulate composite Ep/AS-VF/15,Ep/AS-VF/20,Ep/AS-F/15 and Ep/AS-C/15 ,has damping factor 0.1667,0.11530,0.15909 and 0.1304. This shows that Ep/AS-F and Ep/AS-VF have a better damping factor than Ep/AS-C in 15-20 % weight fraction because the void is created due to agglomeration, which increases the damping capacity of these composites.

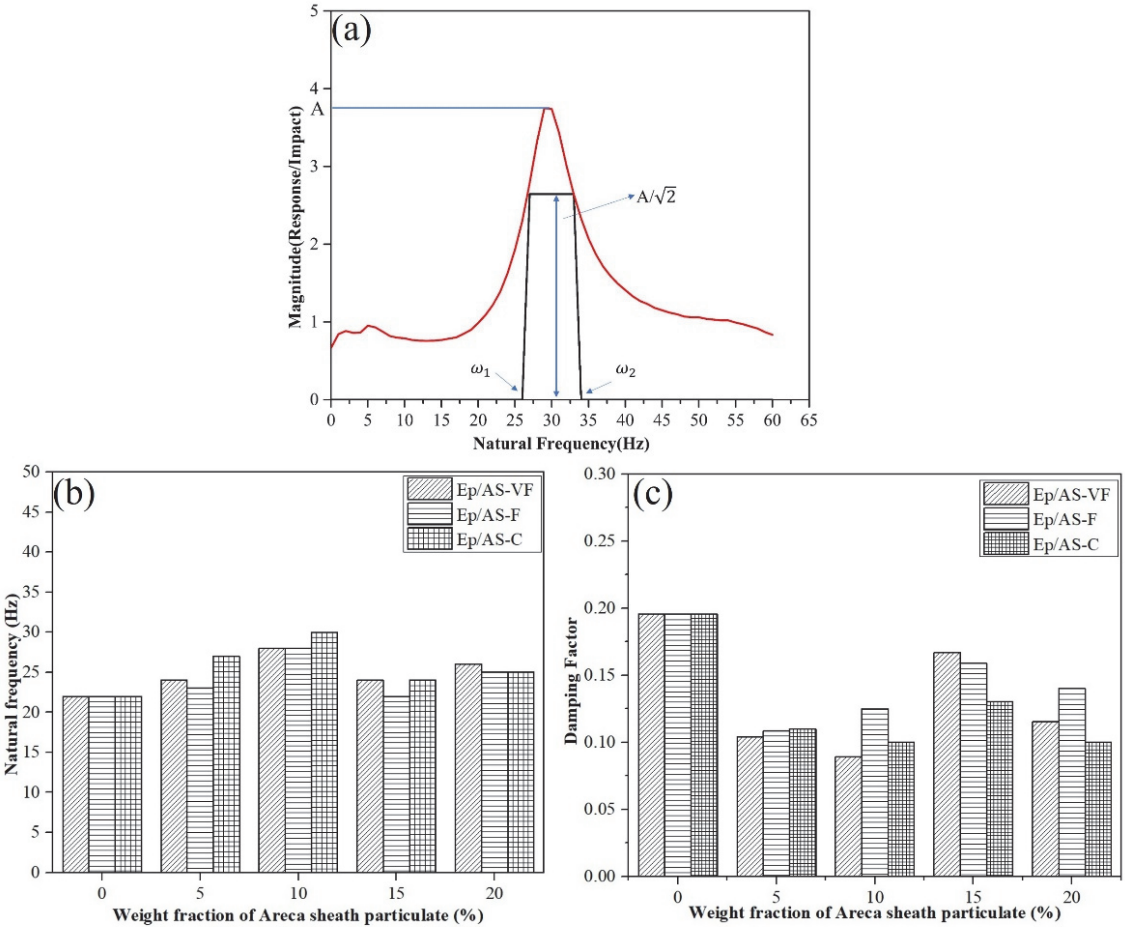

Figure 14: (a)Frequency response function (FRF) of Ep/AS-C/20 (b) Natural Frequency (c) Damping factor in Ep/AS composites.

Fractographic analysis of composites

The properties of composites are strongly dependent on the areca sheath particulate weight fraction, particulate size, and particulate distribution in epoxy resin. The fracture morphology analysis of the areca sheath particulate composites after tensile tests, obtained by scanning electron microscopy ZESIS, EVO MA18, Germany is presented in Fig.15. In Fig.15(a), the control specimen's fractured surface is very smooth, and the river lining pattern specifies that the fractured specimens are brittle. Therefore, the control specimen reveals a brittle fracture behavior. It can be observed that in Fig.15(b), the areca sheath particulate embedded in the epoxy resin, there is no evidence of areca sheath particulate debonding, which suggests the relatively strong bonding, but in Fig.15(c) specimen, the interfacial debonding and void formation occurs this might be due to less wettability of areca sheath particulates. The resin-rich zone was observed in a low weight fraction of areca sheath composites (as shown in Fig. 15(d) and (e)). The fractured surfaces are smoothly aligned, and scraps were observed. This indicates that the tensile strength of these specimens has decreased compared to the control. However, in Fig.15(f), AS-VF agglomerated up to several higher microns is observed. Besides, the void is also observed in the fractured surface, which

may be caused by gas entrapped during manufacturing. The agglomeration of areca sheath particulate and the microstructure defects might explain the decrease in the tensile modulus of Ep/AS-VF/20.

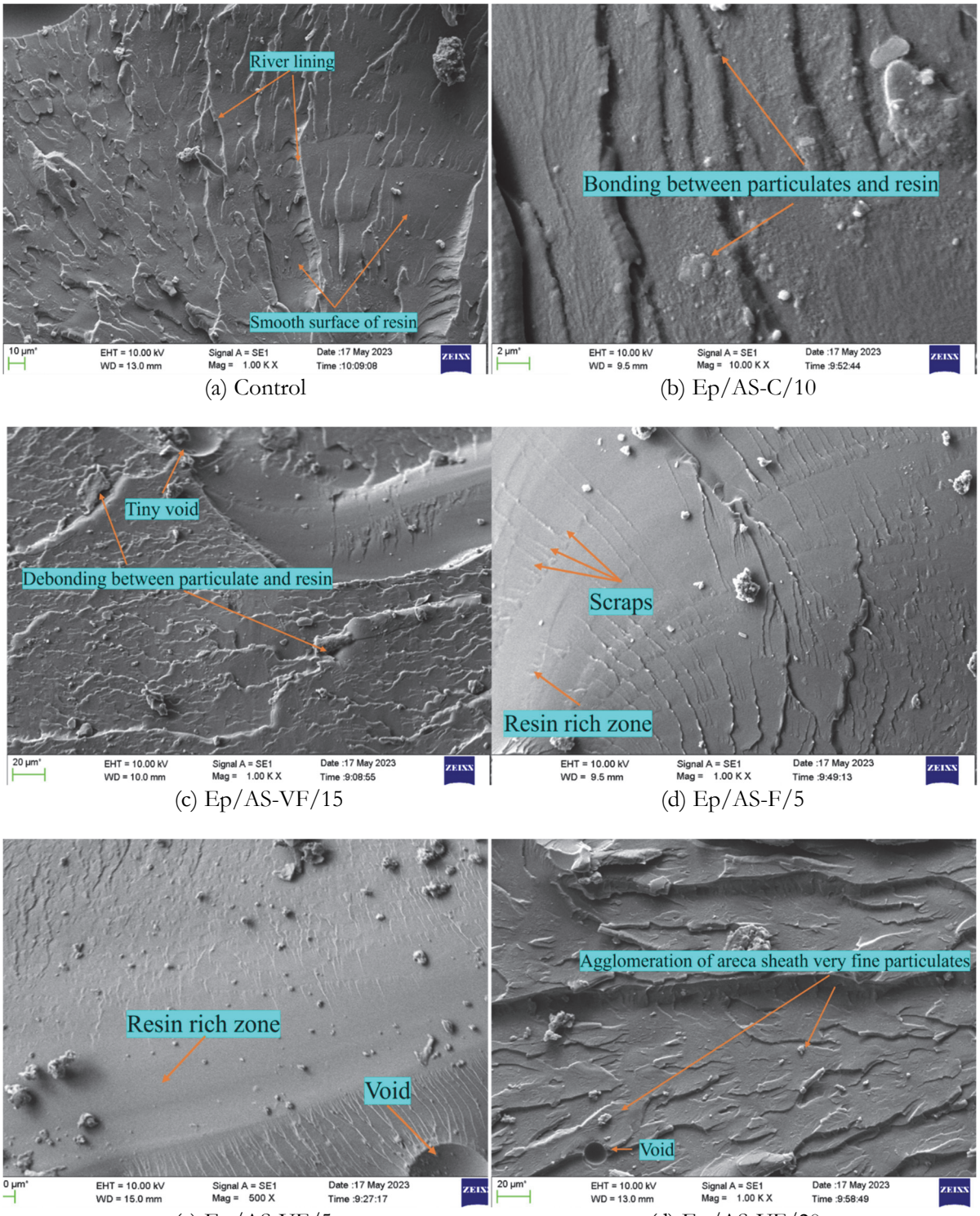

(a) Control (b) Ep/AS-C/10

(c) Ep/AS-VF/15 (d) Ep/AS-F/5

(c) Ep/AS-VF/5 (d) Ep/AS-VF/20

Figure 15: SEM images of a tensile fractured surface.

Composites	Particle Size (μm)	Filler Content %	Tensile Strength (MPa)	Flexural Strength (MPa)	Impact Strength KJ/m2	Hardness (N/mm2)	Ref.
E+Sal	300	33	13.9	44.23	3.2	-	[14]
E+Teak	300	33	14.2	48.92	3.7	-	[14]
E+Pine	(150-300)	25	18.2	20.03	2.2	232.7	[33]
E+Shorea robusta	(150-300)	25	21.8	38.58	20	191.1	[33]
HDPE +Fiberboard	-	40	13.8	31.4	-	-	[34]
E+Apple shell	212	15	45.6	78.19	-	-	[22]
PP+Popular	250	30	22.8	-	9.7 J/m	-	[35]
Phenolic+Cedar	<160	40	34.5	61.82	9.7 J/m	-	[36]
PP+Pine	215	40	25.5	42.6	79 J/m	-	[23]
PP+Pine	64	40	24.30	41.40	91 J/m	-	[18]
Polyester+Grewia	90	30	24.78	66.2			[37]
Present Work (Ep/AS-C/10)	(300-600)	10	24	29.28	54.7 J/m	85.8(SD)	
Present Work (Ep/AS-C/10)	(150-300)	5	14.48	37.99	25.65 J/m	84(SD)	

Table 2: Representative plot of mechanical properties of composites as a filler content.

Property Map

Tab. 2 presents data on the mechanical properties of various composite materials, which are fabricated by combining different types of particles (fillers) with polymer resin. The table highlights several key parameters: particle size, filler content, tensile strength, flexural strength, impact strength, and hardness. The particle sizes of the fillers used in the composites, as detailed in the table, range from 64 μm to 600 μm, significantly impacting the mechanical properties of the materials.
Shakuntala et al. found that a 15-weight fraction % of apple shell-reinforced epoxy composite, with a particle size of 212 μm, had the highest tensile and flexural strength. Conversely, Narlioglu et al. reported the lowest tensile and flexural strength in a 33-weight fraction % Fiberboard HDPE composite. In this study, an Ep/AS-C/10 showed a tensile and flexural strength that falls between the strengths of these two composites, indicating its potential for use in low-load building applications, Partition panels, Ceiling Panels, and similar applications. However, a notable issue with these particulate composites is that grinding the reinforcement to the microscale results in uneven particle sizes, which diminishes the load transfer capacity from the resin to the reinforcement. Moreover, the composite material does not possess the necessary mechanical properties for high-load applications.

CONCLUSION

The epoxy composites with areca sheath particulates ranging from 5 to 20% weight fraction were prepared. The study demonstrates that Ep/AS-C, significantly improve mechanical properties. The optimal tensile strength 24 MPa and modulus 1050 MPa were observed at a 10% weight fraction in the Ep/AS-C/10 composite. The highest flexural modulus 3043 MPa and impact energy 54.7 J/m were recorded in the Ep/AS-C/5 and Ep/AS-C/10 composites. However, adding more than 10% particulates AS-C,F,VF led to a decline in tensile and flexural properties due to agglomeration and poor wettability. The Ep/AS-C/10 specimen exhibited the highest natural frequency 30 Hz . The composites also showed excellent hardness, with a maximum value of 88 shore D for Ep/AS-C/20. These lightweight composites are promising alternatives to wood-based epoxy materials and are well-suited for low-load structural applications, including building panels and infrastructure like Partition panels, Ceiling Panels, and similar applications.

FUNDING

This research received no specific grant from any funding agency in the public, commercial, or not-for-profit sectors.

CONFLICT OF INTEREST

The authors declare that they have no conflict of interest.

NOMENCLATURE SECTION

Each specimen was labeled as Ep/AS-C/5 (Ep/AS stands for Epoxy/Areca Sheath, C stands for coarse, and 5 indicates the weight fraction of the areca sheath. The details of all 12 specimens with different particulates are shown in Tab. 3.

Specimen	Resin	Particulate	Weight fraction
Ep/AS-C/5	Epoxy	Areca Sheath-Coarse	5
Ep/AS-C/10	Epoxy	Areca Sheath-Coarse	10
Ep/AS-C/15	Epoxy	Areca Sheath-Coarse	15
Ep/AS-C/20	Epoxy	Areca Sheath-Coarse	20
Ep/AS-F/5	Epoxy	Areca Sheath-Fine	5
Ep/AS-F/10	Epoxy	Areca Sheath-Fine	10
Ep/AS-F/15	Epoxy	Areca Sheath-Fine	15
Ep/AS-F/20	Epoxy	Areca Sheath-Fine	20
Ep/AS-VF/5	Epoxy	Areca Sheath-Very fine	5
Ep/AS-VF/10	Epoxy	Areca Sheath-Very fine	10
Ep/AS-VF/15	Epoxy	Areca Sheath-Very fine	15
Ep/AS-VF/20	Epoxy	Areca Sheath-Very fine	20

Table 3: Detail of Specimens.

REFERENCES

[1] Zhao, J.R., Zheng, R., Tang, J., Sun, H.J., Wang, J. (2022). A mini-review on building insulation materials from perspective of plastic pollution: Current issues and natural fibres as a possible solution, Journal of Hazardous Materials, 438, pp. 129449, DOI: 10.1016/j.jhazmat.2022.129449.

[2] Amin, M.N., Ahmad, W., Khan, K., Ahmad, A. (2022). A Comprehensive Review of Types, Properties, Treatment Methods and Application of Plant Fibers in Construction and Building Materials, Materials, 15(12), pp. 4362, DOI: 10.3390/ma15124362.

[3] Bledzki, A.K., Gassan, J. (1999). Composites reinforced with cellulose based fibres, Progress in polymer science vol. 24. pp.221–274. DOI:10.1016/S0079-6700(98)00018-5

[4] Laverde, V., Marin, A., Benjumea, J.M., Rincón Ortiz, M. (2022). Use of vegetable fibers as reinforcements in cement-matrix composite materials: A review, Construction and Building Materials, 340(7), DOI: 10.1016/j.conbuildmat.2022.127729.

[5] Raj, M., Fatima, S., Tandon, N. (2020). A study of areca nut leaf sheath fibers as a green sound-absorbing material, Applied Acoustics, 169, pp. 107490, DOI: 10.1016/j.apacoust.2020.107490.

[6] Fatima, S., Mohanty, A.R. (2011). Acoustical and fire-retardant properties of jute composite materials, Applied Acoustics, 72(2–3), pp. 108–14, DOI: 10.1016/j.apacoust.2010.10.005.

[7] Rajesh, M., Singh, S.P., Pitchaimani, J. (2018). Mechanical behavior of woven natural fiber fabric composites: Effect of weaving architecture, intra-ply hybridization and stacking sequence of fabrics, Journal of Industrial Textiles, 47(5), pp. 938–59, DOI: 10.1177/1528083716679157.
[8] Kamath, S.S., Sampathkumar, D., Bennehalli, B. (2017). A review on natural areca fibre reinforced polymer composite materials, Ciencia e Tecnologia Dos Materiais, , pp. 106–28, DOI: 10.1016/j.ctmat.2017.10.001.
[9] Yusriah, L., Sapuan, S.M., Zainudin, E.S., Mariatti, M. (2014). Characterization of physical, mechanical, thermal and morphological properties of agro-waste betel nut (Areca catechu) husk fibre, Journal of Cleaner Production, 72, pp. 174–180, DOI: 10.1016/j.jclepro.2014.02.025.
[10] Srinivasan, H., Arumugam, H., A, A.D., Krishnasamy, B., Abdul, A.A., Murugesan, A., Muthukaruppan, A. (2023). Desert cotton and areca nut husk fibre reinforced hybridized bio-benzoxazine/epoxy bio-composites: Thermal, electrical and acoustic insulation applications, Construction and Building Materials, 363, pp. 129870, DOI: 10.1016/j.conbuildmat.2022.129870.
[11] Yan, L., Kasal, B., Huang, L. (2016). A review of recent research on the use of cellulosic fibres, their fibre fabric reinforced cementitious, geo-polymer and polymer composites in civil engineering, Composites Part B: Engineering, 92, pp. 94–132, DOI: 10.1016/j.compositesb.2016.02.002.
[12] Koruk, H., Genc, G. (2018).Acoustic and mechanical properties of luffa fiber-reinforced biocomposites. Mechanical and Physical Testing of Biocomposites, Fibre-Reinforced Composites and Hybrid Composites, Elsevier, pp. 325–341, DOI: 10.1016/B978-0-08-102292-4.00017-5
[13] Shetty, B.P., Naveen, G.J. (2023). Fractography and tensile studies on the effect of different carbon fillers reinforced hybrid nanocomposites, Frattura Ed Integrita Strutturale,vol 17 , pp. 220–232, DOI: 10.3221/IGF-ESIS.66.14.
[14] Jain, N.K., Gupta, M.K. (2018). Hybrid teak/sal wood flour reinforced composites: Mechanical, thermal and water absorption properties, Materials Research Express, 5(12), DOI: 10.1088/2053-1591/aae24d.
[15] Badyankal, P. V., Gouda, P.S.S., Manjunatha, T.S., Maruthi Prashanth, B.H., Shivayogi, B.H. (2023). Realization of mechanical and tribological properties of hybrid banana, sisal, and pineapple fiber epoxy composites using naturally available fillers, Engineering Research Express, 5(1), DOI: 10.1088/2631-8695/acc311.
[16] Anil, K.C., Hemavathi, A.B., Adeebpasha, A. (2023). Mechanical and fractured surface characterization of epoxy/red mud/fly ash/aluminium powder filled hybrid composites for automotive applications, 64, pp. 93–103, DOI: 10.3221/IGF-ESIS.64.06.
[17] Binoj, J.S., Raj, R.E., Daniel, B.S.S., Saravanakumar, S.S. (2016). Optimization of short Indian Areca fruit husk fiber (Areca catechu L.)–reinforced polymer composites for maximizing mechanical properties, International Journal of Polymer Analysis and Characterization, 21(2), pp. 112–122, DOI: 10.1080/1023666X.2016.1110765.
[18] Miah, M.J., Li, Y., Paul, S.C., Babafemi, A.J., Jang, J.G. (2023). Mechanical strength, shrinkage, and porosity of mortar reinforced with areca nut husk fibers, Construction and Building Materials, 363, DOI: 10.1016/j.conbuildmat.2022.129688.
[19] Barczewski, M., Sa, K., Szulc, J. (2019). Application of sun flower husk , hazelnut shell and walnut shell as waste agricultural fillers for epoxy-based composites : A study into mechanical behavior related to structural and rheological properties, 75(2019 January), pp. 1–11, DOI: 10.1016/j.polymertesting.2019.01.017.
[20] Oladele, I.O., Ogunwande, G.S., Taiwo, A.S., Lephuthing, S.S. (2022). Development and characterization of moringa oleifera fruit waste pod derived particulate cellulosic reinforced epoxy bio-composites for structural applications, Heliyon, 8(6), pp. e09755, DOI: 10.1016/j.heliyon.2022.e09755.
[21] Anand, K.J., Ekbote, T. (2024). Optimization of clamshell content for improved properties in bamboo-epoxy composites, Frattura ed Integrità Strutturale, 69, pp. 29–42, DOI: 10.3221/IGF-ESIS.69.03.
[22] Shakuntala, O., Raghavendra, G., Samir Kumar, A. (2014). Effect of filler loading on mechanical and tribological properties of wood apple shell reinforced epoxy composite, Advances in Materials Science and Engineering, 538651, 9, DOI: 10.1155/2014/538651.
[23] Stark, N.M., Service, F., Rowlands, R.E. (2005). Effects of wood fiber characteristics on mechanical properties of wood / polypropylene composites, Wood and Fiber Science, 35(2), 2003. pp. 167-174
[24] Senthil Kumar, K., Siva, I., Jeyaraj, P., Winowlin Jappes, J.T., Amico, S.C., Rajini, N. (2014). Synergy of fiber length and content on free vibration and damping behavior of natural fiber reinforced polyester composite beams, Materials and Design, 56, pp. 379–386, DOI: 10.1016/j.matdes.2013.11.039.
[25] Chandradass, J., Kumar, M.R., Velmurugan, R. (2007). Effect of nanoclay addition on vibration properties of glass fibre reinforced vinyl ester composites, Materials Letters, 61(22), pp. 4385–4388, DOI: 10.1016/j.matlet.2007.02.009.

[26] Krishnasamy, P., Rajamurugan, G., Aravindraj, S., Sudhagar, P.E. (2022). Vibration and Wear Characteristics of Aloevera/Flax/Hemp Woven Fiber Epoxy Composite Reinforced with Wire Mesh and BaSO4, Journal of Natural Fibers, 19(8), pp. 2885–2901, DOI: 10.1080/15440478.2020.1835782.

[27] McCoy, J.D., Ancipink, W.B., Clarkson, C.M., Kropka, J.M., Celina, M.C., Giron, N.H., Hailesilassie, L., Fredj, N. (2016). Cure mechanisms of diglycidyl ether of bisphenol A (DGEBA) epoxy with diethanolamine, Polymer, 105, pp. 243–254, DOI: 10.1016/j.polymer.2016.10.028.

[28] Subramanyam, S.P., Kotikula, D.K., Bennehalli, B., Babbar, A., Alamri, S., Duhduh, A.A., Rajhi, A.A., Kumar, R., Kotecha, K. (2023). Plain-Woven Areca Sheath Fiber-Reinforced Epoxy Composites: The Influence of the Fiber Fraction on Physical and Mechanical Features and Responses of the Tribo System and Machine Learning Modeling, ACS Omega, 9, pp. 8019−8036 DOI: 10.1021/acsomega.3c08164.

[29] Nayak, S., Mohanty, J.R. (2019). Study of Mechanical, Thermal, and Rheological Properties of Areca Fiber-Reinforced Polyvinyl Alcohol Composite, Journal of Natural Fibers, 16(5), pp. 688–701, DOI: 10.1080/15440478.2018.1432000.

[30] Fu, S., Feng, X., Lauke, B., Mai, Y. (2008). Effects of particle size , particle / matrix interface adhesion and particle loading on mechanical properties of particulate – polymer composites, 39, pp. 933–961, DOI: 10.1016/j.compositesb.2008.01.002.

[31] Migneault, S., Koubaa, A., Erchiqui, F., Chaala, A., Englund, K., Wolcott, M.P. (2009). Composites : Part A Effects of processing method and fiber size on the structure and properties of wood – plastic composites, Composites Part A, 40(1), pp. 80–85, DOI: 10.1016/j.compositesa.2008.10.004.

[32] Kuan, H.T.N., Tan, M.Y., Shen, Y., Yahya, M.Y. (2021). Mechanical properties of particulate organic natural filler-reinforced polymer composite: A review, Composites and Advanced Materials, 30, pp. 263498332110075, DOI: 10.1177/26349833211007502.

[33] Khan, M.Z.R., Srivastava, S.K., Gupta, M.K. (2019). Water absorption and its effect on mechanical properties of hybrid wood particulates composites, Materials Research Express, 6(10), DOI: 10.1088/2053-1591/ab34c3.

[34] Narlıoğlu, N., Salan, T., Karaoğul, E., Alma, M.H. (2018). Evaluation of potassium humate material in wood-plastic composite production, Kastamonu Üniversitesi Orman Fakültesi Dergisi, 18(2), pp. 189–202, DOI: 10.17475/kastorman.346857.

[35] Nourbakhsh, A., Karegarfard, A., Ashori, A., Nourbakhsh, A. (2010). Effects of particle size and coupling agent concentration on mechanical properties of particulate-filled polymer composites, Journal of Thermoplastic Composite Materials, 23(2), pp. 169–174, DOI: 10.1177/0892705709340962.

[36] Lette, M.J., Ly, E.B., Ndiaye, D., Takasaki, A., Okabe, T. (2018). Evaluation of Sawdust and Rice Husks as Fillers for Phenolic Resin Based Wood-Polymer Composites, Open Journal of Composite Materials, 08(03), pp. 124–137, DOI: 10.4236/ojcm.2018.83010.

[37] Singha, A.S., Rana, A.K., Jarial, R.K. (2013). Mechanical, dielectric and thermal properties of Grewia optiva fibers reinforced unsaturated polyester matrix based composites, Materials and Design, 51, pp. 924–934, DOI: 10.1016/j.matdes.2013.04.035.